Steel and Composite Structures, *Vol. 25, No. 1* (*2017*) *105-116*
DOI: https://doi.org/10.12989/scs.2017.25.1.105

Ant colony optimization for dynamic stability of laminated composite plates

Erfan Shafei* and Akbar Shirzad

Faculty of Civil Engineering, *Urmia University of Technology*, *Urmia*, *Iran*

(*Received November 04, 2016, Revised April 22, 2017, Accepted June 18, 2017*)

Abstract. This paper presents the dynamic stability study of laminated composite plates with different force combinations and aspect ratios. Optimum non-diverging stacking is obtained for certain loading combination and aspect ratio. In addition, the stability force is maximized for a definite operating frequency. A dynamic version of the principle of virtual work for laminated composites is used to obtain force-frequency relation. Since dynamic stiffness governs the divergence or flutter, an efficient optimization method is necessary for the response functional and the relevant constraints. In this way, a model based on the ant colony optimization (ACO) algorithm is proposed to search for the proper stacking. The ACO algorithm is used since it treats with large number of dynamic stability parameters. Governing equations are formulated using classic laminate theory (CLT) and von-Karman plate technique. Load-frequency relations are explicitly obtained for fundamental and secondary flutter modes of simply supported composite plate with arbitrary aspect ratio, stacking and boundary load, which are used in optimization process. Obtained results are compared with the finite element method results for validity and accuracy convince. Results revealed that the optimum stacking with stable dynamic response and maximum critical load is in angle-ply mode with almost near-unidirectional fiber orientations for fundamental flutter mode. In addition, short plates behave better than long plates in combined axial-shear load case regarding stable oscillation. The interaction of uniaxial and shear forces intensifies the instability in long plates than short ones which needs low-angle layup orientations to provide required dynamic stiffness. However, a combination of angle-ply and cross-ply stacking with a near-square aspect ratio is appropriate for the composite plate regarding secondary flutter mode.

Keywords: ant colony optimization; dynamic stability; flutter; combined force; laminated composite plate

1. Introduction

Aerospace systems have intricate parts with several design variables and limits. For the next generation airliners, it is essential to make use of composite parts in order to reduce the weight and enhance the aero-elastic response. Thus, we need to find design parameters and stacking pattern in order to satisfy design-oriented provisions for composite laminates. Engineers usually trust the experience and similar existing designations in order to determine the unknowns. This can result in a non-optimal designation of aeronautic systems. However, it is necessary to find an optimum stacking of composites in order to ensure their dynamic stability.

The significance of dynamic stability in aerospace design has provided motivation for progress of several research works. Fukuchi and Tanaka (2006) briefed non-periodic motions of circular arch with focus on follower forces. An aerodynamic stability analysis of suspension bridges with structural constrains is available in Zhang (2010). Debowski *et al*. (2010) investigated the dynamic stability of a metal foam rectangular plates analytically using Bubnov-Galerkin method for rectangular plates and compared with the numerical solution. Shafei and Kabir (2011) presented study on dynamic stability of composite plates with focus on rectangular shapes and combined boundary forces. Kurpa *et al*. (2013) studied the nonlinear vibration and stability of thin fiber-reinforced composite laminates plates of subjective quadrilateral geometry with diverse boundary conditions. They proposed a theoretical approach based on the application of the *R*-functions theory and variational methods. Wang *et al*. (2013) studied the hygrothermal effects on the dynamic instability of a laminated composite plate subjected to random pulsating load. Chen *et al*. (2013) presented the dynamic stability analysis of laminated composite plates in thermal environments with focus on temperature, layer number, modulus ratio, and load parameters.

Later, the axisymmetric dynamic instability of polar orthotropic sandwich annular plate with electrorheological damping treatment is investigated by Yeh (2014). Dey *et al*. (2015) presented a generic random model representations approach for free vibration analysis of angle-ply composite plates. Najafov *et al*. (2014) investigated the stability of exponentially graded (EG) cylindrical shells with shear stresses on a Pasternak foundation and obtained the expressions for critical hydrostatic pressures based on classic laminate theory (CLT). Sofiyev and Kuruoglu (2015) studied the effects of non-homogeneity, anisotropy, and geometrical parameters on the values of the critical plate load. Lecheb *et al*. (2015) predicted the fatigue life of composite wind turbine blade under dynamic loads with follower forces. Sabuncu *et al*. (2016) studied the static and dynamic stability of cracked multi-story steel frames.

*Corresponding author, Assistant Professor,
E-mail: e.shafei@uut.ac.ir

ISSN: 1229-9367 (Print), 1598-6233 (Online)

Biswal *et al*. (2016) investigated the hygrothermal effects on free vibration of woven fiber glass/epoxy laminated composite cylindrical shallow shells based on the first order shear deformation theory (FSDT).

In this way, recent works are conducted with focus on the optimization of composite plates. Hajianmaleki and Qatu (2013) conducted studies on the structural optimization of straight and curved composite beams. Aydin *et al*. (2016) and Ehsani and Rezaeepazhand (2016) investigated the optimization of composite plate for high stiffness and buckling force using genetic algorithm. Ho-Huu *et al*. (2016) optimization the stacking of laminated composite plates to maximize buckling load using differential evolution. Stability of hat-stringer-stiffened composite flat panel subjected to axial compression was investigated by Mo *et al*. (2016) and optimization was done to get an optimal cross section. In advance, Sreehari and Maiti (2016) enhanced the buckling load of damaged composite plates in hygrothermal environment using unified particle swarm optimization. Guimaraes *et al*. (2017) analyzed the panel flutter and optimization of composite tow steered plates. Hu *et al*. (2017) predicted the performance of fiber-reinforced composite plates using and optimization of uncertain design parameters. Maalawi (2017) introduced a mathematical model to maximize the natural frequencies and minimize vibration amplitudes of thin-walled functionally graded box beams with closed cross-sections. Finally, Roque and Martins (2017) used differential evolution optimization to find staking sequences for maximization of the natural frequency of symmetric and asymmetric laminates.

Based on the recent studies, the optimization of laminated composite plates becomes a complex problem with constraints on the dynamic stability performance of aerospace structures. Multiple parameters affect the instability force and result in vibrations with modal shifts. Most aircrafts and spacecraft structures deform under aerodynamic forces in which the force combinations change in time. This amplifies the combined force effect on the dynamic stability of composite plates. Thus, instability force of composite plates needs to be maximized for a predefined vibration frequency.

Current work presents an analytical procedure for design of a slender composite plate. It is intended to design a plate to resist maximum force prior to instability while it is vibrating with a definite frequency. The optimum design geometry and stacking is achieved by means of ant colony optimization (ACO) technique, which is one of the well-known meta-heuristics and do not need to express the objective function in an explicit way.

Since plates resist combined axial and shear forces in their boundaries, it is necessary to consider the combination of forces and the subsequent effect on dynamic stability. Interest is a stable dynamic response with the maximum resisted force. Stable dynamic response is non-diverging oscillation, denoted as flutter, within a definite force value and combination. Study considers straight, rectangular, thin-walled composite plate with combined boundary forces and geometric aspect ratios. Analysis variables are number of plies (n_p), ply orientation (θ_p), bidirectional force ratio (ξ), shear force ratio (η) and plate aspect ratio (γ). The ACO algorithm is used to solve the nonlinear optimization problem. The goal is to find the laminate stacking, plate aspect ratio, and the load combination ratio for stable dynamic response all assumed as variables using the ACO technique rather than cases as Aymerich and Serra (2008), Wang *et al*. (2010), Shafei and Kabir (2011), and Awad *et al*. (2012) in which at least one parameter is kept constant. The difference between current research work and existing researches is that the ACO method is employed for dynamic stability applications and the energy formulation is used to consider the total stiffness terms, which some of them are neglected in PDE formulation. Another innovation is that the appropriate plate aspect ratio and force combination are determined for flutter with maximum resisted load subjected to the interaction between bidirectional axial and shear forces.

2. Materials and methods

2.1 Analytical formulation

Symmetrically laminated composite plate with A domain in $x-y$ coordinates and axial-shear boundary forces as shown in Fig. 1 is assumed. For transverse displacement in the fixed coordinate$w(x.y.t)$,the Hamilton's principle for the piece of plate in time domain

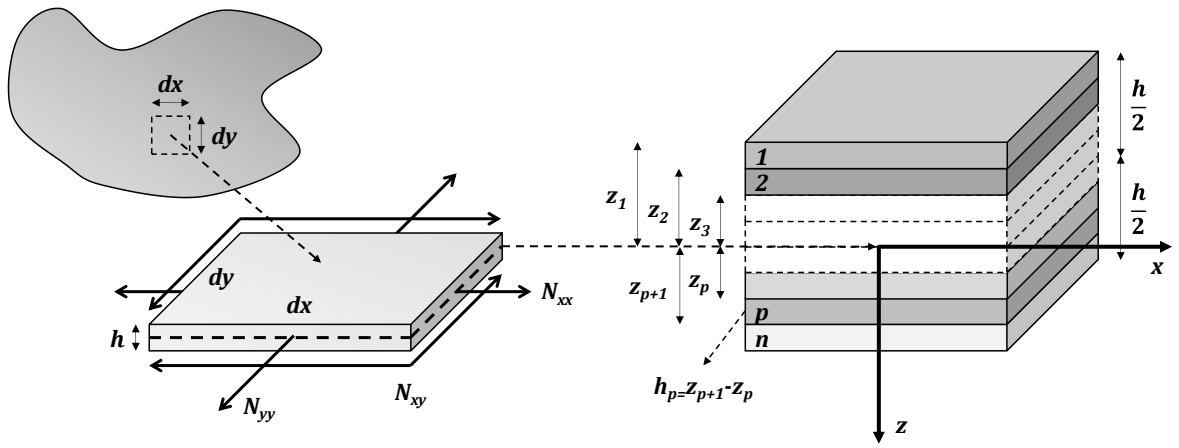

Fig. 1 Integrated elemental forces for a laminated composite plate and layered section

$t_i \le t < t_f$ leads to the familiar variational form as Eq. (1).

$$\delta \int_{t_i}^{t_f} (U + W - T)dt = 0 \tag{1}$$

Here, U is the total strain energy due to bending of the plate, W is the external of in-plane forces on the transverse deflection, and T is the kinetic energy of structural mass. In addition, t_i and t_f define the arbitrary time domain considered for equilibrium. The CLT can be applicable for formulation of problem as rectangular composite plates have sufficiently large aspect ratios and do not have major cutouts through. The strain energy U for a symmetrically laminated thin plate in CLT is as Eq. (2)

$$\begin{aligned} U = \frac{1}{2}\int_0^a \int_0^b \Bigg[& D_{11}\left(\frac{\partial^2 w}{\partial x^2}\right)^2 + D_{22}\left(\frac{\partial^2 w}{\partial y^2}\right)^2 \\ & +2D_{12}\left(\frac{\partial^2 w}{\partial x^2}\right)\left(\frac{\partial^2 w}{\partial y^2}\right) + D_{66}\left(\frac{\partial^2 w}{\partial x \partial y}\right)^2 \\ & +4D_{16}\left(\frac{\partial^2 w}{\partial x^2}\right)\left(\frac{\partial^2 w}{\partial x \partial y}\right) \\ & +4D_{26}\left(\frac{\partial^2 w}{\partial y^2}\right)\left(\frac{\partial^2 w}{\partial x \partial y}\right)\Bigg] dydx \end{aligned} \tag{2}$$

where, a and b are the length and width of rectangular plate, respectively. Stiffness coefficients, D_{ij}, for a laminate consisting of n_p orthotropic layers and h_k ply height from mid-plane are as Eq. (3).

$$D_{ij} = \frac{1}{3}\sum_{k=1}^{n_p} Q_{ij}^k (z_k^3 - z_{k-1}^3) \tag{3}$$

Here, Q_{ij}^k is an orthotropic in-plane stiffness term of k^{th} ply in laminate. These coefficients vary from layer to layer and depend on the material properties and orientation of the layer. The external work due to in-plane boundary forces is as Eq. (4).

$$\begin{aligned} W = \frac{1}{2}\int_0^a \int_0^b \Bigg[& N_{xx}\left(\frac{\partial w}{\partial x}\right)^2 + N_{yy}\left(\frac{\partial w}{\partial y}\right)^2 \\ & +2N_{xy}\left(\frac{\partial w}{\partial x}\right)\left(\frac{\partial w}{\partial y}\right)\Bigg] dydx \end{aligned} \tag{4}$$

In which, N_{xx} and N_{yy} are edge-normal distributed forces with positive sign for tension in each direction and N_{xy} is the distributed shear force. The kinetic energy, T, for the rectangular plate domain is as Eq. (5).

$$T = \frac{1}{2}\int_0^a \int_0^b \rho h\left(\frac{\partial w}{\partial t}\right)^2 dydx \tag{5}$$

where, ρ is the average density of the composite material and h is the total thickness of laminate. Planar vibrations are neglected for the simplicity of analysis. It is assumed that the boundaries are simply supported and the distributed forces are uniform along edges. The eigenvalue solution of problem is in form of Eq. (6).

$$\begin{aligned} & w(x.y.t) \\ & = \sum_{m=1}^{\infty}\sum_{n=1}^{\infty} W_{mn}\left(e^{\frac{im\pi}{a}x} - e^{-\frac{im\pi}{a}x}\right)\left(e^{\frac{in\pi}{b}y} - e^{-\frac{in\pi}{b}y}\right)e^{i\omega t} \end{aligned} \tag{6}$$

Here, W_{mn} is the vibration amplitude, ω is the angular frequency of the vibration, and m and n are the wave number in x and y directions, respectively. Although the characteristic form of displacement solution obtained from Strum-Liovielle theorem is of interest, it is necessary to derive the general solution so that it would be independent of the wave numbers. The general closed-form solution of the problem is as Eq. (7) using von-Karmen plate technique.

$$\begin{aligned} w(x.y.t) = \{ & C_1 e^{p(x+y)} + C_2 e^{q(x+y)} + C_3 e^{p(x-y)} \\ & + C_4 e^{q(x-y)} + C_5 e^{p(-x+y)} + C_6 e^{q(-x+y)} \\ & + C_7 e^{p(-x-y)} + C_8 e^{q(-x-y)}\} e^{i\omega t} \end{aligned} \tag{7a}$$

$$p = \sqrt{\frac{\beta + 2\omega\sqrt{\rho h}}{4\alpha}} \;.\; q = \sqrt{\frac{\beta - 2\omega\sqrt{\rho h}}{4\alpha}} \tag{7b}$$

The $C_1 . \cdots . C_8$ coefficients are vibration amplitude constants and depend on the boundary conditions of composite plate. It should be noted that the obtained solution is valid for all plate cases and has to satisfy the assumed boundary conditions in this study. The simply-supported plate has the following curvature-deflection conditions.

$$w(0.y.t) = w(a.y.t) = w(x.0.t) = w(x.b.t) = 0 \tag{7c}$$

$$\begin{aligned} & \frac{\partial^2 w}{\partial x^2}(0.y.t) = \frac{\partial^2 w}{\partial x^2}(a.y.t) \\ & = \frac{\partial^2 w}{\partial y^2}(x.0.t) = \frac{\partial^2 w}{\partial y^2}(x.b.t) = 0 \end{aligned} \tag{7d}$$

The Eq. (7a) function is the solution of both buckling and vibration Eigen problems. However, the case that both phenomena exist is concerned in current study. Applying boundary conditions of Eq. (7c) and Eq. (7d) into solution and solving for $C_1 . \cdots . C_8$ coefficients gives the Eq. (6) solution. However, p and q variables need to be expressed as functions of geometric and mechanical properties of plate. For this purpose, boundary condition-satisfied solution is substituted in Eq. (1) to give unknown parameters. This substitution leads to Eq. (8) relation set.

$$\alpha = D_{11} + D_{22} + 2(D_{12} + 2D_{66}) + 4(D_{16} + D_{26}) \tag{8a}$$

$$\beta = -\left(D_{11}N_{xx} + N_{yy}D_{22} + 2(D_{12} + 2D_{66})N_{xy}\right) \tag{8b}$$

Here, α and β are parametric material and geometric

stiffness terms of laminate. Here, the β factor is formulated as negative for compressive forces acting in boundaries as the dynamic instability is considered. In this procedure, the flexural stiffness terms are considered completely which improves the accuracy of further results. The interaction between compression and shear force results in negative geometric stiffness and subsequent dynamic instability in element with infinitesimal curvature. After simplifications, the frequency of the first two modes will be as Eq. (9). The governing flutter will be the load combination, which makes modes to occur simultaneously.

$$\{\rho h\omega^2 a^4 b^4 + K_1 - K_2\} \times \{\rho h\omega^2 a^4 b^4 + 4K_1 - 16K_2\} = \frac{4096}{81} a^6 b^6 \left[N_{xy} - 10\pi^2 \left(\frac{D_{16}}{a^2} + \frac{D_{26}}{b^2}\right)\right]^2 \tag{9a}$$

$$K_1 = \pi a^2 b^2 \left[N_{yy}\, a^2 + N_{xx}\, b^2\right]$$
$$K_2 = \pi^4 [D_{11} b^4 + D_{22} a^4 + 2a^2 b^2 (D_{12} + 2D_{66})] \tag{9b}$$

For further simplification, N_{yy} and N_{xy} forces are expressed as ξN_{xx} and ηN_{xx}, respectively. The load combination may lead to either flutter or divergence. Increasing the load level with compressive stress field effect decreases the overall stiffness of element and may lead to either flutter or divergence depending on internal restoration load. Flutter is denoted for cases in which the internal load overcomes the vibration acceleration and the dynamic equilibrium is satisfied. When the restoration load is not high enough to control the vibration, the acceleration of structure increases without definite rate and leads to instability called as divergence. The first step is to solve the above relation with respect to N_{xx} to obtain the critical flutter force. The solution of the aforementioned equation is as Eq. (10).

$$\omega_1^2 = \frac{1}{18\rho h a^4 b^4}\left[9(17K_2 - 5K_1) + \sqrt{K_3}\right] \tag{10a}$$

$$\omega_2^2 = \frac{1}{18\rho h a^4 b^4}\left[9(17K_2 - 5K_1) - \sqrt{K_3}\right] \tag{10b}$$

$$K_3 = 729(K_1 - 5K_2)^2 + 16384\left(a^3 b^3 N_{xy} - 10\pi^2 ab(b^2 D_{16} + a^2 D_{26})\right)^2 \tag{10c}$$

Equating ω_1^2 and ω_2^2 results to the fundamental flutter force, N_{xx}^f. This is the case when the K_3 constant is zero. Therefore, the flutter force is as Eq. (11) after some simplifications.

$$N_{xx}^f = \frac{135\pi^4 [b^4 D_{11} - a^4 D_{22}]}{27(\pi ab)^2 (b^2 - \xi a^2) + 128\eta a^3 b^3} \tag{11}$$

It is notable that above flutter force has a critical value for ξ parameter when η is set to zero. This means that lateral compression has decreasing effect on the longitudinal flutter force and may result in divergence. However, the shear force can stabilize the negative effect of lateral force and improve the flutter force. The flutter frequency, ω_f^2, is as Eq. (12) after substitution of Eq. (11) into Eq. (10). The divergence response occurs when ξ tend to critical value.

$$\omega_f^2 = \frac{27\pi^6 [4b^6 D_{11} - 4a^6 D_{22}\xi + T_1 + T_2]}{\rho h a^4 b^4 [27\pi^2 (\xi a^2 - b^2) - 128\eta ab]} - \frac{64\eta ab\pi^4 [16a^2 b^2 (D_{12} + 2D_{66}) + T_3]}{\rho h a^4 b^4 [27\pi^2 (\xi a^2 - b^2) - 128\eta ab]} \tag{12}$$
$$T_1 = a^2 b^4 [21 D_{11}\xi - 8(D_{12} + 2D_{66})]$$
$$T_2 = a^4 b^2 [8\xi (D_{12} + 2D_{66}) - 21 D_{22}]$$
$$T_3 = \left(17 + 15\sqrt{2}\right) b^4 D_{11} + \left(17 - 15\sqrt{2}\right) a^4 D_{22}$$

In order to investigate the second unstable flutter mode, the third and fourth mode frequency is obtained as below equation solved for ω.

$$\{\rho h\omega^2 a^4 b^4 + K_3 - K_5\} \times \{\rho h\omega^2 a^4 b^4 + K_4 - K_6\} = \frac{4096}{81} a^6 b^6 \left[N_{xy} - 10\pi^2 \left(\frac{D_{16}}{a^2} + \frac{D_{26}}{b^2}\right)\right]^2 \tag{13a}$$

$$K_3 = \pi a^2 b^2 \left[N_{yy}\, a^2 + 4N_{xx}\, b^2\right]$$
$$K_4 = \pi a^2 b^2 \left[4N_{yy}\, a^2 + N_{xx}\, b^2\right]$$
$$K_5 = \pi^4 [16 D_{11} b^4 + D_{22} a^4 + 8a^2 b^2 (D_{12} + 2D_{66})]$$
$$K_6 = \pi^4 [D_{11} b^4 + 16 D_{22} a^4 + 8a^2 b^2 (D_{12} + 2D_{66})] \tag{13b}$$

Terms K_3 and K_4 are denoted as modal geometric stiffness terms of higher modes. In addition, K_5 and K_6 are compound modal stiffness of plate and are related to convergence of adjacent vibration modes. The solution of third and fourth frequencies, ω_3^2 and ω_4^2 results in the following second flutter force, N_{xx}^s, after simplification.

$$N_{xx}^s = \frac{135\pi^4 [b^4 D_{11} + a^4 D_{22} + 2a^2 b^2 (D_{12} + 2D_{66})]}{27(\pi ab)^2 (b^2 + \xi a^2) + 128\eta a^3 b^3} \tag{14}$$

The secondary flutter force defines another interaction between biaxial compression and shear forces. Here, the shear and biaxial compression forces stabilize the vibration of plate and secondary flutter phenomenon depends on the bending-shear stiffness terms. The secondary flutter frequency, ω_s^2, is as Eq. (15).

$$\omega_s^2 = T_4 \frac{b^4 D_{11} + a^4 D_{22} + 2a^2 b^2 (D_{12} + 2D_{66})}{\rho h a^4 b^4 [27\pi^2 (\xi a^2 + b^2) + 128\eta ab]} \tag{15}$$
$$T_4 = 4\pi^4 \left[16\left(17 + 15\sqrt{2}\right) ab\eta - 27\pi^2 (\xi a^2 + b^2)\right]$$

Flutter loads and matching frequencies of all other converging modes can be calculated by means of setting zero the determinant of equilibrium equation coefficient array. The advantage of current approach is that an explicit solution for fundamental flutter mode can be obtained and so the objective function in optimization process can be directly defined.

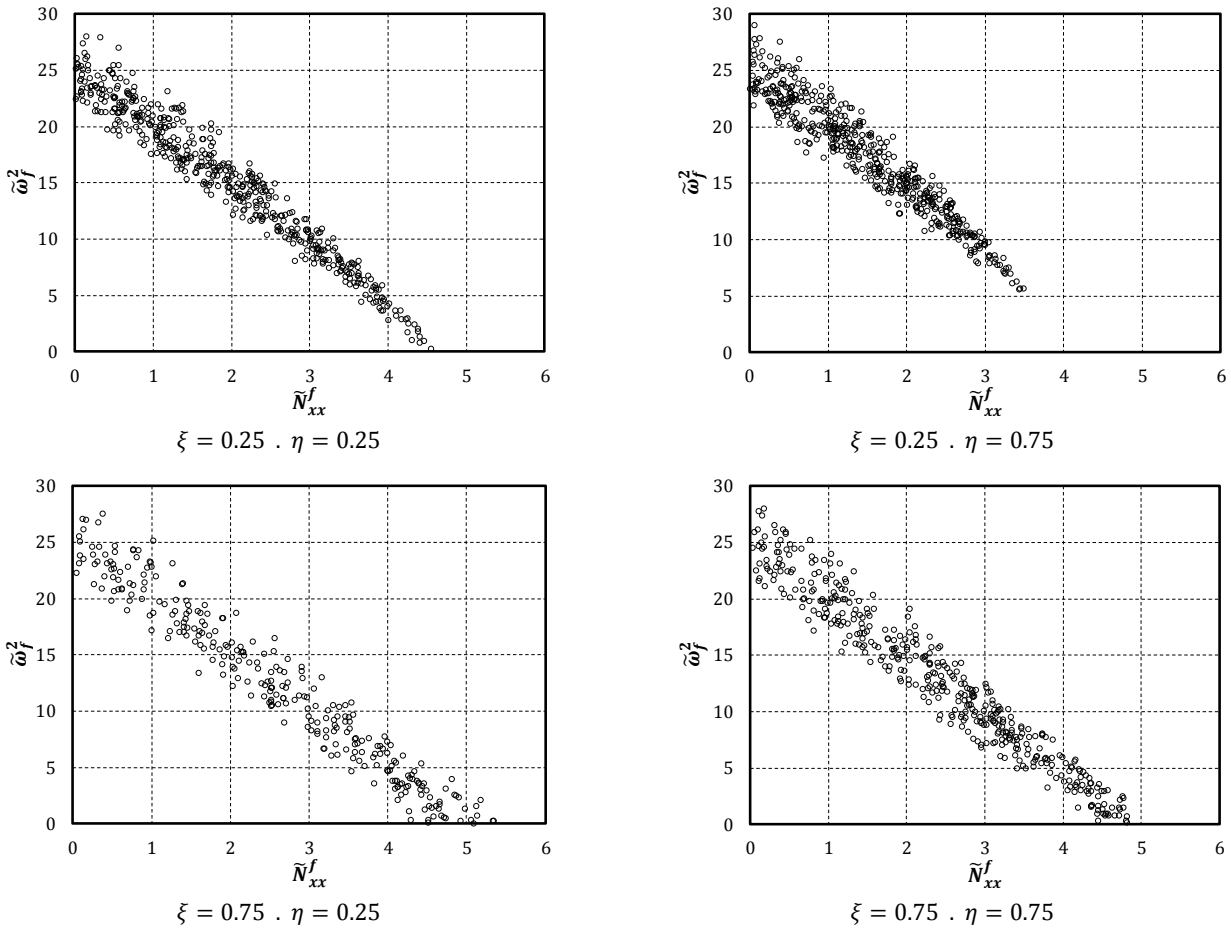

Fig. 2 The scatter of non-dimensional fundamental flutter frequency versus force

2.2 Response assessment

The primary step is to investigate if an optimum design case is available for the problem. It is necessary to evaluate the flutter force and frequency to detect the aspect of the solution and provide an algorithm to find the optimum case. For this purpose, a glass fabric material with fiber modulus, $E_{11} = 55$ GPa, matrix modulus, $E_{22} = 9.5$ GPa, shear modulus, $G_{12} = 5.5$ GPa, Poisson's ratio, $\mu_{12} = 0.33$, and mass density, $\rho = 1.6 \times 10^{-9}$ ton/mm^3, is assumed for analysis. Primarily an 8-ply laminate with 0.125 mm ply thickness and random fiber orientation in each ply is assumed to generate an illustration case to show the response. Number of plies, orientation, plate aspect ratio and loading combinations will be determined further using optimization method of the interest optimum case. Non-dimensional flutter frequency, $\tilde{\omega}_f^2$, and corresponding force, $\tilde{N}_{xx}^f$, is defined as following for explanation of results.

$$\tilde{N}_{xx}^f = N_{xx}^f \frac{a^2}{\pi^2 D_{11}} \tag{16a}$$

$$\tilde{\omega}_f^2 = \omega_f^2 \frac{\rho h a^4}{\pi^4 D_{11}} \tag{16b}$$

Fig. 2 shows the flutter frequency, $\tilde{\omega}_f^2$, versus the corresponding force, $\tilde{N}_{xx}^f$, for various load combination ratios, ξ, and η, of square composite plate, $a = b$. Results show that the lateral compression decreases the flutter load and frequency. There exist less feasible stable design cases for load combination as $\xi = 0.75$ and $\eta = 0.25$. For this case, the [+45°|+35°|+25°|-30°]$_s$ and [-45°|-45°|+40°|+40°]$_s$ layups have minimum and maximum flutter forces, respectively. However, shear force improves the flutter cases and makes it possible to happen. It is notable that all assumed cases are possible and feasible as a design for $\xi = 0.25$ and $\eta = 0.75$ load combinations. Here, [+05°|±00°|-05°|+10°]$_s$ and [+45°|+35°|+85°|+15°]$_s$ layups have the minimum and maximum flutter forces, correspondingly. Therefore, it is necessary to find the load combination with maximum flutter force.

FEM models consist of S8 double curvature linear shell elements with Full-Gaussian quadrate integration. Numerical FEM analyses consist of nonlinear geometric procedure with application of boundary forces followed by eigenvalue procedure for solution of vibration frequencies.

Nonlinear geometric procedure takes into account the reduced stiffness of plate for eigenvalue vibration analysis. The flutter frequencies of FEM approach are obtained using successive mesh refinements up to desired convergence with relative error less than 1×10^{-4} is achieved. Fig. 3 shows the flutter mode shape of plates that are taken from numerical analysis. The flutter frequencies of considered cases are reported in Table 1, which shows the correlation

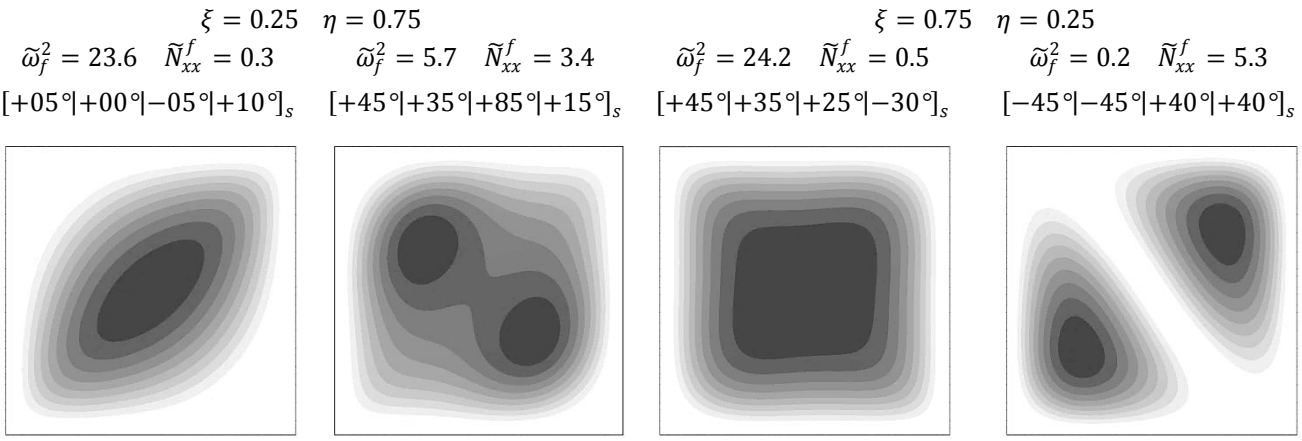

Fig. 3 Flutter modes of square composite plate in numerical analysis

Table 1 Comparison of analytical and numerical values of non-dimensional flutter frequency ($\widetilde{\omega}_f^2$)

Case	Layup	FEM (Abaqus®)	Analytical (Eqs. (11) and (12))	Logarithmic error
1	$[+05°\|\pm00°\|-05°\|+10°]_s$	25.62	23.6	-1.10
2	$[+45°\|+35°\|+85°\|+15°]_s$	6.14	5.7	-1.14
3	$[+45°\|+35°\|+25°\|-30°]_s$	23.35	24.2	-1.34
4	$[-45°\|-45°\|+40°\|+40°]_s$	0.22	0.2	-1.04

between FEM and analytical results. As show in this table, logarithmic estimation error is -1.04, which corresponds to 9.1% relative error and is in acceptable range for a simplified analytical solution.

Based on the primarily obtained results, it is essential to determine the layup for a maximum flutter force regarding the appropriate load combination and plate aspect ratio. The case with maximum flutter force for a predefined vibration frequency will be an optimum design. For this purpose, an optimization procedure is developed to express the design aspects of the plate.

2.3 Ant Colony Optimization (ACO) Procedure

In this section, the ant colony optimization (ACO) technique is used to search for the optimum designation. The optimum case is defined as a plate with the maximum flutter force when it is excited under a definite vibration frequency. ACO is a meta-heuristic algorithm based on the behavior of real ants in finding the shortest path from their nest to food sources as described in Kaveh and Bakhshpoori (2015) and Hu and Fish (2016) research works. There are various types of ACO. One of them is known as the best iteration ant system (AS_{ib}) as described in Phan *et al.* (2012). This algorithm is an enhanced version of the initially proposed ant system (AS) algorithm. In the present study, AS_{ib} is used for optimization of N_{xx}^f flutter force. The parameters of the AS_{ib} are m as the number of ants, α as the weight of pheromone, β as the weight of local heuristics, τ_0 as the initial pheromone, φ as the pheromone reward factor, HV as the heuristic value, ρ as the pheromone persistence parameter, PV as the penalty function value and $It_{\max}$ as the maximum iteration number. Fig. 4 shows the computational flowchart of the AS_{ib}. Readers are referred to the paper proposed by Stützle and Hoos (2000) for more details about the AS_{ib}.

2.4 Feasibility space discretization

The decision variables are load combination factors, ξ & η, plate aspect ratio, $\gamma = a/b$, number of plies, n_p, and ply angle, θ_p. The practical range for decision variables are selected as Table 2 for optimization process. Therefore, the size of decision space will be 2.061×10^{22}. To demonstrate the capability of ACO technique, the case previously studies by Librescu and Thangjitham (1991) and Krishnamurthy (2010) is selected for initial validation and calibration of the operating frequency for optimization problem. Plate is subjected to combined forces $N_{xx}^f(t) = N_{xx}^f \sin(\widetilde{\omega}_f^0 t)$, $N_{yy}^f(t) = \xi N_{xx}^f \sin(\widetilde{\omega}_f^0 t)$, and $N_{xy}^f(t) = \eta N_{xx}^f \sin(\widetilde{\omega}_f^0 t)$ with constant flutter frequency of $\widetilde{\omega}_f^0 = 487$ rad/sec.

Reported value is assumed for plate part design of wing to resist dynamic instability. Study aims to find a special stacking sequence and number of plies to maximize the flutter load for the studied cases. The objective is to maximize the N_{xx}^f flutter force for a plate with width (b) of 1000 mm. The number of plies, ply orientation, plate aspect ratio, and load combination ratios are assumed as variables is ACO optimization procedure. The detail of objective function is as Eq. (17) and the constraint is as Eq. (18).

$$Objective\ Function: F = N_{xx}^f - PF \tag{17}$$

$$Constrained\ to: \widetilde{\omega}_f = \widetilde{\omega}_f^0 \tag{18}$$

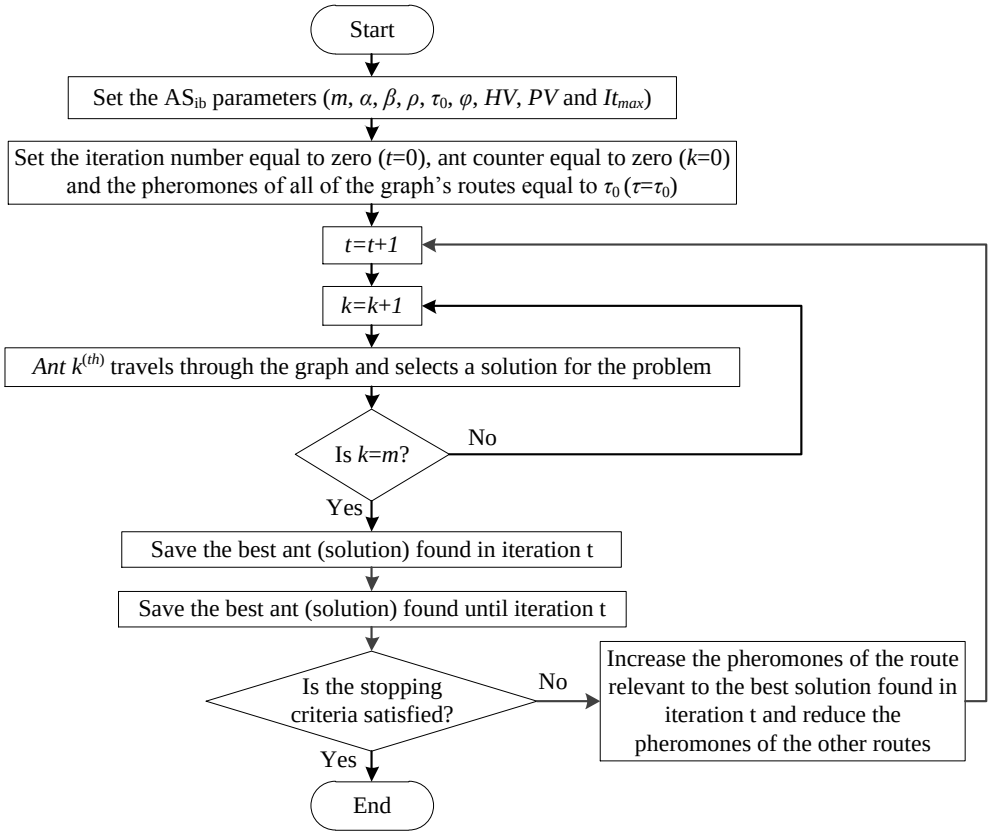

Fig. 4 Computational flowchart of the AS_{ib} in ACO technique

where, F is the objective function, N_{xx}^{f} is the flutter force and PF is the penalty function and is calculated as Eq. (16).

$$PF = PV \times \begin{cases} \left(0.95 \times \tilde{\omega}_f^0\right) - \tilde{\omega}_f & if\ \tilde{\omega}_f < \left(0.95 \times \tilde{\omega}_f^0\right) \\ N_{xx}^{f} & if\ N_{xx}^{f} > 0\ and\ \tilde{\omega}_f^0 < 0 \\ \tilde{\omega}_f - \left(1.05 \times \tilde{\omega}_f^0\right) & if\ \tilde{\omega}_f > \left(1.05 \times \tilde{\omega}_f^0\right) \\ 0 & otherwise \end{cases} \quad (19)$$

The value of PV is selected rationally large number as the arbitrary guess of the ACO algorithm is not in the feasible range and tends to small numbers not greater than 1×10^{-4} when the iterations converge to a constant answer for the problem. The PV term is used to force stochastic iterations to fit the solution in the feasible target domain.

3. Results and discussions

3.1 Fundamental flutter mode

Current section presents the results acquired using optimization method and compares them with the existing database. The applicability of the presented method can be measured up on the new layups which provide adequate flutter stiffness. Primarily, it is necessary to conduct sensitivity analysis and calibrate the ACO technique. Table 3 shows the parameters of AS_{ib} achieved by sensitivity analysis. The maximum dynamic force, N_{xx}^{f}, determined by AS_{ib} is 0.9855 N/mm. Table 4 presents the details of this optimum solution.

Table 2 Selectable values considered for decision variables

ξ	η	γ	n_p	θ_p
0.0	0.0	0.25	1	-90
0.1	0.1	0.30	2	-75
0.2	0.2	0.35	3	-60
0.3	0.3	0.40	4	-45
0.4	0.4	0.45	5	-30
0.5	0.5	0.50	6	-15
0.6	0.6	0.55	7	0
0.7	0.7	0.60	8	15
0.8	0.8	0.65	9	30
0.9	0.9	0.70	10	45
1.0	1.0	0.75	11	60
		0.80	12	75
		0.85	13	90
		0.90	14	
		0.95	15	
		1.0	16	

Fig. 4 shows the convergence curve of AS_{ib}. According to this figure, AS_{ib} finds the optimum solution after 643 iterations. It is notable that the solution layup [+15|+30|

Table 3 Parameters of AS_{ib} obtained by sensitivity analysis

Parameter	Value
α	1.0
β	0.9
τ_0	5
HV	1
ρ	0.99
m	120
φ	100
PV	1000

Table 4 Details of the best solution obtained by AS_{ib} for fundamental flutter mode

$N_{xx}^{f.\mathrm{Max}}\ (N/mm)$	0.9855
Number of objective function evaluations	77078
ξ	0.0
η	1.0
γ	0.35
n_p	16
$[+15°\|+30°\|-30°\|+30°\|-30°\|-15°\|+15°\|-30°]_s$	

-30|+30|-30|-15|+15|-30]$_S$ is a special 16-ply angle-ply. Librescu and Thangjitham (1991) are proposed thicker angle-plies to achieve stability, which approves the validity of the current solution.

In this section, the stability and possible flutter mode shapes of the optimum designation is investigated in order to determine the aspects of the response. Thus, a numerical model is presented to simulate the vibration of the optimized plate for the fundamental unstable mode. A plate with 1000 mm width and 350 mm length with characteristics stated in Table 4 in modeled. The optimized layup is [+15°|+30°|-30°|+30°|-30°|-15°|+15°|-30°]$_s$ that is subjected to uniaxial compression and shear forces simultaneously. The magnitudes of boundary dynamic forces, N_{xx} and N_{xy}, are $0.9855\ \mathrm{N/mm}$ that is estimated as maximum critical force. In order to validate the optimization results, the vibration frequencies of the first two modes are extracted. Fig. 6 shows the finite element model used for analysis.

It is expected that the first two modes have the same oscillation frequency equal to 77.5 Hz as constrained in the calculation procedure. However, there will be difference between two modes as they are coincident in the maximized dynamic force. Fig. 6 shows the vibration modes of plate in optimized case. As shown in figure, there exist two different

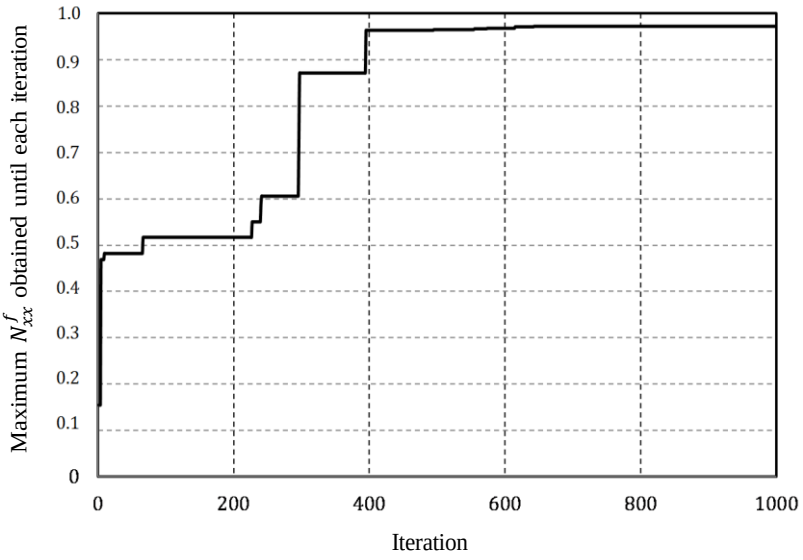

Fig. 5 Convergence curve of the AS_{ib} during the optimi-zation process

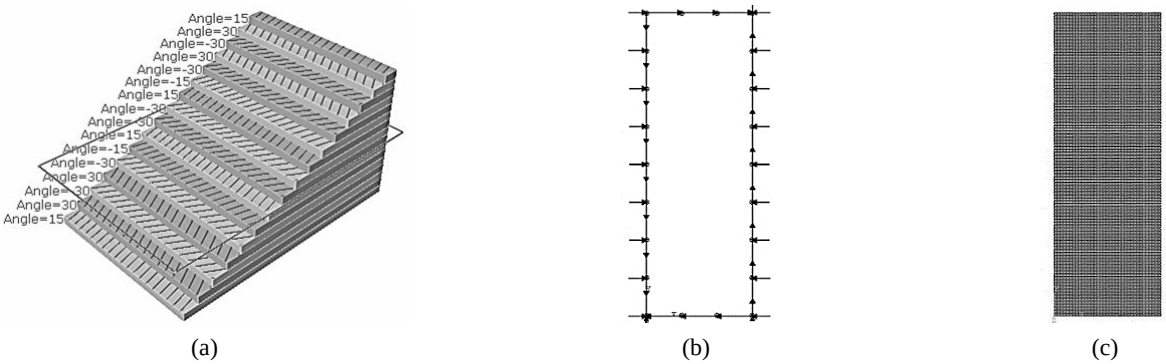

(a) (b) (c)

Fig. 6 Configuration of optimized plate: (a) ply stacking; (b) boundary loading; (c) meshing

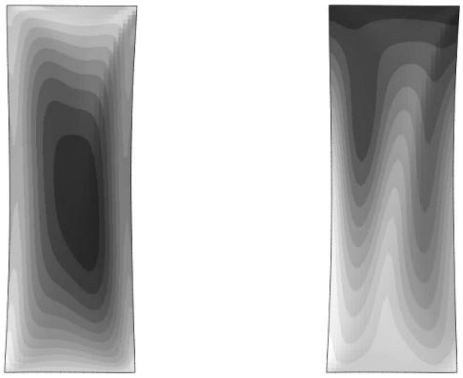

(a) 1st mode (b) 2nd mode

Fig. 7 Configuration of optimized plate: (a) ply stacking; (b) boundary loading; (c) meshing

vibration modes for a constant dynamic force and frequency in fundamental unstable stage.

As shown in this figure, the first mode has the peak deflection in the middle of plate. However, the second mode has lateral sliding deformation. It is the case in which the axial and shear flutter modes occur simultaneously. On the other hand, the fundamental flutter frequency is obtained as 77.6 Hz, which is very close to the predefined value and approves the validity of the proposed optimization model. For further description of the ACO technique, the calculation steps are reported in Table 5, which shows the pattern of AS_{ib} decision parameters.

Based on the obtained results, the convergence rate of AS_{ib} in primary parameters is high with respect to conventional optimization methods. The dynamic force ratios are determined in initial stages of procedure and ACO continues to test various orientation angles. It is notable that the AS_{ib} finds the optimum stacking for the case when there is not lateral compression for plate and shear load is present simultaneously. In addition, the optimized plate has $\gamma = 0.35$ aspect ratio, which is practical for aspect proportioning of aerospace parts. Here, shear force improves the dynamic stiffness of the plate for fundamental unstable mode and improves the maximum critical force value. Therefore, it is recommended to use angle-ply type laminate for the case where there is combination of compression and shear forces. Optimum laminate has almost-unidirectional plies in top, middle and bottom in order to resist longitudinal compression. However, angle-plies with orientation of $\pm 30°$ are used between unidirectional plies to provide shear stiffness. Since the optimized laminate has angle-plies in the 1st-quarter and 3rd-quarter of its thickness, it can be assumed as a predefined orientation for plates, which has to resist dynamic forces. In advance, the ACO is used to determine the appropriate plate aspect ratio, stacking, thickness, and force combination regarding secondary unstable mode.

Table 6 Details of the best solution obtained by AS_{ib} for secondary flutter mode

$N_{xx}^{s.Max}\ (N/mm)$	1.6465
Number of objective function evaluations	98776
ξ	0.2
η	0.6
γ	0.85
n_p	12
$[+90°\|+30°\|+75°\|0°\|+30°\|+90°\|-60°]_s$	

3.1 Secondary flutter mode

In this section, the ACO technique is applied for the secondary unstable vibration of laminated composite plate to find the appropriate stacking, aspect ratios, and load combination. The parameters of AS_{ib} achieved by sensitivity analysis in the fundamental mode are also assumed for the second mode to minimize the numerical error. The secondary maximum dynamic force, N_{xx}^{s}, estimated by AS_{ib} is 1.6465 N/mm, which is larger than N_{xx}^{f}. Table 6 presents the details of this optimum solution. The AS_{ib} finds the secondary optimum solution after 542 iterations, which is comparable to the iterations made for fundamental solution. It is observed that the plate resists the maximum dynamic force when biaxial compression is combined with shear if optimum solutions of fundamental and secondary modes are compared. Here, the optimum plate has an aspect ratio near to square case with lower number of plies than the previous case. Thus, a thinner plate with appropriate aspect ratio will resist the dynamic forces only if the fundamental flutter is restrained.

The optimized plate is composed of cross-ply and angle-ply in top-bottom and middle of the thickness, respectively. Unlike the previous case where 16-ply angle-ply layup is required for fundamental flutter mode, a 14-ply combination of cross-ply and angle-ply is appropriate for maximum secondary flutter mode. It is notable that the current optimum layup is determined for the previously assumed flutter frequency. However, the pattern of stacking would be almost the same for other flutter frequencies. It is essential

Table 5 Details of the solution stages in AS_{ib} for fundamental flutter mode

Itr.	Layup	n_p	ξ	η	γ	$N_{xx}^{f.\max}$ (N/mm)
66	$[+45°\|+30°\|-15°\|-60°\|0°\|+15°\|+75°]_s$	14	0.0	0.9	0.35	0.5240
297	$[+30°\|0°\|-15°\|-60°\|+90°\|-90°\|+90°\|+45°]_s$	16	0.0	1.0	0.35	0.8834
395	$[-30°\|+30°\|+15°\|-15°\|-15°\|-30°\|-45°\|+45°]_s$	16	0.0	1.0	0.35	0.9768
495	$[+15°\|+30°\|-30°\|+15°\|+45°\|+30°\|-45°\|-30°]_s$	16	0.0	1.0	0.35	0.9784
555	$[+15°\|-30°\|+30°\|+30°\|-30°\|0°\|-45°\|-90°]_s$	16	0.0	1.0	0.35	0.9802
643	$[+15°\|+30°\|-30°\|+30°\|-30°\|-15°\|+15°\|-30°]_s$	16	0.0	1.0	0.35	0.9855

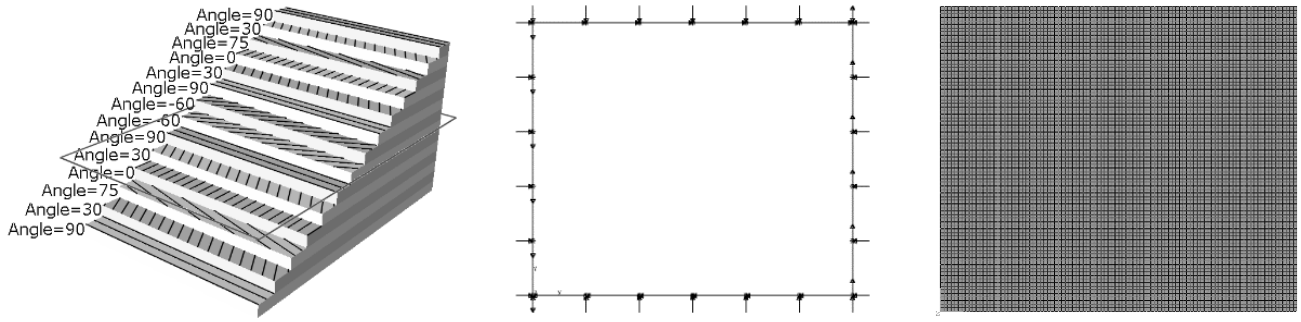

(a) (b) (c)

Fig. 8 Configuration of optimized plate: (a) ply stacking; (b) boundary loading; (c) meshing

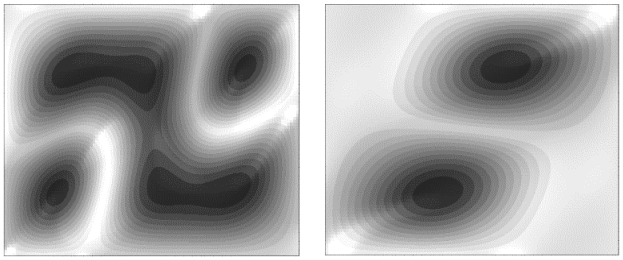

(a) (b)

Fig. 9 Vibration modes of the optimized composite plate for the secondary unstable case

to present a numerical simulation in order to validate the obtained results of the optimized plate for the secondary flutter mode. The width, height, and thickness of the simulated plate are 1000 mm, 850 mm, and 1.75 mm, respectively. The magnitudes of N_{yy}, and N_{xy} are 0.3293 N/mm and 0.9879 N/mm, respectively. The vibration frequencies of the first and second modes are extracted using FEA. Fig. 8 shows the FEM model used for simulation.

Fig. 9 shows the vibration modes of plate in optimized case. As shown in figure, there exist also two different oscillation modes in secondary flutter mode with a single vibration frequency. The vibration shape shows the complex interaction between biaxial compression and shear forces.

Unlike the vibration shape of optimized plate for fundamental flutter mode, the peak deflection of current plate is maximum along a diagonal path for the second flutter mode and is not uniform. Flutter mode of the plate in composed of the combination of biaxial compression and shear modes and has the frequency of 77.6 Hz as major and secondary modes are obtained for a constant external vibration frequency. The calculation steps of secondary flutter mode are reported in Table 7 that shows the outline of AS_{ib} decision parameters.

Here, the convergence rate of AS_{ib} in primary parameters is higher that the fundamental mode. The plate aspect ratio, load combination and number of plies are determined in primary steps of analysis and only iterations are made for ply orientations. It is notable that the aspect ratio optimized plate is near to unit since such a designation is appropriate for plates with high stiffness for dynamic forces. Based on the obtained results, it is recommended to use angle-ply with 30° and 60° angles in middle and cross-ply in top-bottom of thickness to resist the maximum force in secondary flutter mode. Similar to the results of previous section, angle-plies are used between cross-plies to perform the best. Therefore, it can be assumed as a predefined orientation for composite plates subjected to dynamic forces. The ACO method determines the aspect ratio, load combination factors and layup number in the primary stages of the optimization process. However, the extensive effort is made on the stacking orientation search, which has a large decision space (equal to 13^{16}). Although the searching priority of all parameters is the same, the efficiency of ACO is measured on the ply orientations.

4. Conclusions

Current research provides a mathematical approach for the flutter analysis of the composite plates subjected to combined in-plane dynamic forces. Ant colony optimization technique is used in combination of analytical solution to search for an optimum plate design with maximum critical

Table 7 Details of the solution stages in AS_{ib} for secondary flutter mode

Itr.	Layup	n_p	ξ	η	γ	$N_{xx}^{f.\max}$ (N/mm)
56	$[0°\|\text{-}15°\|+60°\|+30°\|+45°\|+45°]_s$	12	0.1	0.5	0.85	0.8754
250	$[\text{-}90°\|0°\|+15°\|+15°\|\text{-}60°\|\text{-}60°\|+90°]_s$	14	0.2	0.5	0.35	1.4759
333	$[\text{-}90°\|+45°\|+45°\|0°\|\text{-}30°\|\text{-}90°\|+45°]_s$	14	0.2	0.6	0.35	1.6319
417	$[+90°\|+30°\|+75°\|0°\|+30°\|\text{-}90°\|0°]_s$	14	0.2	0.6	0.35	1.6346
468	$[+90°\|+30°\|+65°\|0°\|+30°\|+75°\|\text{-}60°]_s$	14	0.2	0.6	0.35	1.6377
542	$[+90°\|+30°\|+75°\|0°\|+30°\|+90°\|\text{-}60°]_s$	14	0.2	0.6	0.35	1.6465

dynamic force. Plate aspect ratio, thickness, ply orientation, and boundary force ratio are selected as decision parameters in optimization procedure. The optimum stacking and related parameters are determined for fundamental and secondary flutter modes. The validity and accuracy of results are checked using finite element models of the optimum designs regarding external forces and vibration frequencies. Based on the extracted results, the optimum plate aspect ratio and ply orientation depend of the interaction between shear and biaxial compression, which control the geometric stiffness of plate. Conclusions of the current study can be abbreviated as following points:

- It is possible to find a thinner stacking by means of advanced optimization techniques, which can provide the required stiffness to resist in-plane dynamic forces.
- Ant colony optimization is efficient in optimum stacking search and it rapidly tends to the solution. Although the governing equations are nonlinear function of ply orientation, this procedure provides practical solution that is used in present design.
- Regarding fundamental flutter mode, the optimum stacking is angle-ply with unidirectional plies in the top, middle and bottom of thickness. Still, optimization results recommend use of rectangular plates with one-third aspect ratios to maximize the critical dynamic force.
- For the secondary flutter mode, the ant colony optimization suggests an almost-square plate with angle-ply and cross-ply in middle and top-bottom of the thickness, respectively.
- The stability of fundamental flutter mode is function of uniaxial compression and shear interaction. However, simultaneous biaxial compression and shear forces lead to higher critical force for secondary flutter mode.

References

Abaqus Inc. (2007), ABAQUS 6.7 User's Manual; Simulia, Johnston, RI, USA.

Awad, Z.K., Aravinthan, T., Zhuge, Y. and Gonzalez, F. (2012), "A review of optimization techniques used in the design of fiber composite structures for civil engineering applications", *Mater. Des.*, **33**, 534-544.

Aydin, L., Aydin, O., Artem, H.S. and Mert, A. (2016), "Design of dimensionally stable composites using efficient global optimization method", *Proceedings of the Institution of Mechanical Engineers, Part L: Journal of Materials Design and Applications*, 1464420716664921.

Aymerich, F. and Serra, M. (2008), "Optimization of laminate stacking sequence for maximum buckling load using the ant colony optimization (ACO) metaheuristic", *Compos. Part A: Appl. Sci. Manuf.*, **39**(2), 262-272.

Biswal, M., Sahu, S.K. and Asha, A.V. (2016), "Vibration of composite cylindrical shallow shells subjected to hygrothermal loading-experimental and numerical results", *Compos. Part B: Eng.*, **98**, 108-119.

Chen, C.S., Tsai, T.C., Chen, W.R. and Wei, C.L. (2013), "Dynamic stability analysis of laminated composite plates in thermal environments", *Steel Compos. Struct., Int. J.*, **15**(1), 57-79.

Debowski, D., Magnucki, K. and Malinowski, M. (2010), "Dynamic stability of a metal foam rectangular plate", *Steel Compos. Struct., Int. J.*, **10**(2), 151-168.

Dey, S., Mukhopadhyay, T. and Adhikari, S. (2015), "Stochastic free vibration analysis of angle-ply composite plates–a RS-HDMR approach", *Compos. Struct.*, **122**, 526-536.

Ehsani, A. and Rezaeepazhand, J. (2016), "Stacking sequence optimization of laminated composite grid plates for maximum buckling load using genetic algorithm", *Int. J. Mech. Sci.*, **119**, 97-106.

Fukuchi, N. and Tanaka, T. (2006), "Non-periodic motions and fractals of a circular arch under follower forces with small disturbances", *Steel Compos. Struct., Int. J.*, **6**(2), 87-101.

Guimaraes, T.A., Castro, S.G., Rade, D.A. and Cesnik, C.E. (2017), "Panel flutter analysis and optimization of composite tow steered plates", *Proceedings of the 58th AIAA/ASCE/AHS/ASC Structures, Structural Dynamics, and Materials Conference*, Grapevine, TX, USA, January, 1118.

Hajianmaleki, M. and Qatu, M.S. (2013), "Vibrations of straight and curved composite beams: A review", *Compos. Struct.*, **100**, 218-232.

Ho-Huu, V., Do-Thi, T.D., Dang-Trung, H., Vo-Duy, T. and Nguyen-Thoi, T. (2016), "Optimization of laminated composite plates for maximizing buckling load using improved differential evolution and smoothed finite element method", *Compos. Struct.*, **146**, 132-147.

Hu, N. and Fish, J. (2016), "Enhanced ant colony optimization for multiscale problems", *Computat. Mech.*, **57**(3), 447-463.

Hu, X.B., Cui, X.Y., Liang, Z.M. and Li, G.Y. (2017), "The performance prediction and optimization of the fiber-reinforced composite structure with uncertain parameters", *Compos. Struct.*, **164**, 207-218.

Kaveh, A. and Bakhshpoori, T. (2015), "Subspace search mechanism and cuckoo search algorithm for size optimization of space trusses", *Steel Compos. Struct., Int. J.*, **18**(2), 289-303.

Krishnamurthy, T. (2010), "Frequencies and flutter speed estimation for damaged aircraft wing using scaled equivalent plate analysis", *Proceedings of the 51st AIAA/ASME/ASCE/AHS/ASC Structures, Structural Dynamics, and Materials Conference 18th AIAA/ASME/AHS Adaptive Structures Conference 12th* (p. 2769), Orlando, FL, USA, April.

Kurpa, L., Mazur, O. and Tkachenko, V. (2013), "Dynamical stability and parametrical vibrations of the laminated plates with complex shape", *Latin Am. J. Solids Struct.*, **10**(1), 175-188.

Lecheb, S., Nour, A., Chellil, A., Mechakra, H., Ghanem, H. and Kebir, H. (2015), "Dynamic prediction fatigue life of composite wind turbine blade", *Steel Compos. Struct., Int. J.*, **18**(3), 673-691.

Librescu, L. and Thangjitham, S. (1991), Analytical studies on static aeroelastic behavior of forward-swept composite wing structures", *J. Aircraft*, **28**(2), 151-157.

Maalawi, K.Y. (2017), "Dynamic optimization of functionally graded thin-walled box beams", *Int. J. Struct. Stabil. Dyn.*, 1750109.

Mason, B., Stroud, W., Krishnamurthy, T., Spain, C. and Naser, A. (2005), "Probabilistic design of a wind tunnel model to match the response of a full-scale aircraft", *Proceedings of the 46th AIAA/ASME/ASCE/AHS/ASC Structures, Structural Dynamics and Materials Conference*, Austin, TX, USA, April, 2185.

Mo, Y., Ge, D. and He, B. (2016), "Experiment and optimization of the hat-stringer-stiffened composite panels under axial compression", *Compos. Part B: Eng.*, **84**, 285-293.

Najafov, A.M., Sofiyev, A.H., Hui, D., Karaca, Z., Kalpakci, V. and Ozcelik, M. (2014), "Stability of EG cylindrical shells with shear stresses on a Pasternak foundation", *Steel Compos. Struct., Int. J.*, **17**, 453-470.

Phan, D.T., Lim, J.B., Tanyimboh, T.T. and Sha, W. (2012), "An efficient genetic algorithm for the design optimization of cold-formed steel portal frame buildings", Ph.D. Thesis; Michigan State University, East Lansing, MI, USA.

Roque, C.M.C. and Martins, P.A.L.S. (2017), "Maximization of fundamental frequency of layered composites using differential evolution optimization", *Compos. Struct.* DOI: j.compstruct.2017.01.037

Sabuncu, M., Ozturk, H. and Yashar, A. (2016), "Static and dynamic stability of cracked multi-story steel frames", *Struct. Eng. Mech., Int. J.*, **58**(1), 103-119.

Shafei, E. and Kabir, M.Z. (2011), "Dynamic Stability Optimization of Laminated Composite Plates under Combined Boundary Loading", *App. Compos. Mater.*, **18**(6), 539-557.

Sofiyev, A.H. and Kuruoglu, N. (2015), "Buckling of non-homogeneous orthotropic conical shells subjected to combined load", *Steel Compos. Struct., Int. J.*, **19**(1), 1-19.

Sreehari, V.M. and Maiti, D.K. (2016), "Buckling load enhancement of damaged composite plates under hygrothermal environment using unified particle swarm optimization", *Struct. Multidiscipl. Optimiz.*, **55**(2), 437-447.

Stützle, T. and Hoos, H.H. (2000), "MAX–MIN ant system", *Future Gener. Comput. Syst.*, **16**(8), 889-914.

The Math Works, Inc. (2005), MATLAB 7.04 User's Manual; Mathworks, Natick, MA, USA.

Wang, W., Guo, S., Chang, N. and Yang, W. (2010), "Optimum buckling design of composite stiffened panels using ant colony algorithm", *Compos. Struct.*, **92**(3), 712-719.

Wang, H., Chen, C.S. and Fung, C.P. (2013), "Hygrothermal effects on dynamic instability of a laminated plate under an arbitrary pulsating load", *Struct. Eng. Mech., Int. J.*, **48**(1), 103-124.

Yeh, J.Y. (2014), "Axisymmetric dynamic instability of polar orthotropic sandwich annular plate with ER damping treatment", *Smart Struct. Syst., Int. J.*, **13**(1), 25-39.

Zhang, X.J. (2010), "Study of structural parameters on the aerodynamic stability of three-tower suspension bridge", *Wind Struct., Int. J.*, **13**(5), 471-485.

CC